1.4 Investigation of Horizontal Vibrations on Marangoni Convection in a Liquid Bridge

Masahiro Kawaji
University of Toronto

INVESTIGATION OF HORIZONTAL VIBRATIONS ON MARANGONI CONVECTION IN A LIQUID BRIDGE

M. Kawaji, M. Nasr-Esfahany and S. Simic

Dept. of Chemical Engineering and Applied Chemistry, 200 College Street, Toronto, Ontario M5S 3E5, Canada

Abstract

An experimental investigation has been conducted on Marangoni convection in liquid bridges of 7 mm diameter with acetone (Pr = 4.3) and 5 cSt silicone oil (Pr = 67) to investigate the temperature oscillation characteristics and the effects of small horizontal vibrations on the onset of oscillatory flow and surface dynamics. For acetone, the temperature oscillation frequency increased nearly linearly with the disk temperature difference, but inversely with the aspect ratio. For the partially open system, the oscillation frequencies were about 20% greater than those determined for the closed system at the same ΔT. The variation of the temperature oscillation frequency with ΔT was in qualitative agreement with that predicted previously by a numerical simulation.

Vibration experiments were conducted with acetone, water and silicone oil bridges, by applying horizontal vibrations of different amplitudes and frequencies. For an isothermal water bridge, the surface oscillation amplitude was found to be strongly dependent on the volume ratio of the liquid bridge, and the oscillation frequency was much larger than the frequency of the vibrations applied. A previous vibration model for a straight cylinder was modified to predict the vibration frequency of a hyperboloid-shaped liquid bridge. The predictions of the modified model showed qualitative agreement with the measurements.

For acetone and silicone oil bridges, vibrations of different amplitudes and frequencies were applied to determine their effects on the critical temperature difference. For increasing the temperature difference, ramp and step increase methods were used for acetone and silicone oil bridges, respectively. For a vibrating liquid bridge, a step increase method was found to be more appropriate for obtaining more accurate critical ΔT data. The critical temperature difference was then measured for acetone and silicone oil bridges vibrated at different acceleration levels, but no apparent effect of vibration could be observed on the critical temperature difference in the ranges of variables covered. The response of the liquid bridge surface was also recorded by a video camera and the surface motion was analyzed for different volume and aspect ratios. Greater amplitudes of surface vibration were measured when the disk temperature difference was greater than the critical value compared to an isothermal liquid bridge. The surface oscillation amplitude was also found to increase with the distance below the hot corner.

1. INTRODUCTION

Marangoni convection in liquid bridges has attracted a significant amount of interest in the past, mainly due to the use of a floating zone process to fabricate single semiconductor crystals of high purity from melts. In order to enhance the efficiency and feasibility of this

crystal growth process, large liquid bridges with a large diameter are desired, which can be obtained under microgravity in space.[1] It is well known that when a large temperature gradient is imposed, Marangoni convection changes from a steady, axi-symmetric flow to an oscillatory flow, leading to non-uniformities in crystal structure such as striations.[2] In microgravity environment aboard a space platform, liquid bridges are also susceptible to small vibrations or g-jitter, that may excite oscillations of the free surface and add to the complexity of the hydrodynamics involved.

Previously, many experiments performed on Marangoni convection in liquid bridges have indicated that the critical Marangoni number, at which steady to oscillatory flow transition occurs, varies with the Prandtl number, disk diameter, volume ratio and aspect ratio of the liquid bridge. The critical temperature difference, ΔT_{cr}, and the frequency of temperature oscillations for a disk diameter of 6 mm at various aspect ratios have been measured for high temperature melts (KCl and $NaNO_3$).[3, 4] Triple coupling among the velocity, temperature and surface deformation was suggested to be responsible for transition from steady, axi-symmetric to oscillatory flow in high Pr fluids.[5]

The effect of surface evaporation has been investigated in preceding years using acetone, which is volatile and causes significant mass and heat transfer at the free surface. It became clear that evaporation has a stabilizing effect on the onset of oscillatory Marangoni convection in an evaporating liquid bridge. The effect of small horizontal vibrations on the liquid bridge shape was also investigated without any temperature gradient imposed. Also, a *horizontal vibration model* of Ichikawa et al. [6] was adopted to predict the resonance vibration frequency of the liquid bridge.

In this work, the temperature oscillation data obtained previously for acetone bridge were analyzed to investigate the dependence of oscillation frequency on the disk temperature difference, ΔT. New experiments were also conducted to study the effect of horizontal vibrations on the shape of a water bridge without any temperature gradient and Marangoni convection in acetone and silicone oil liquid bridges. The vibration characteristics of water liquid bridge have also been investigated without imposing any temperature gradient. The conventional way of ramping up the temperature difference between the disks to determine the critical temperature difference, ΔT_{cr}, was replaced by a new method involving step changes in temperature difference to get more precise ΔT_{cr} data for the case where an external vibration was imposed on the liquid bridge. With the main focus on vibration or g-jitter effects, surface oscillation characteristics were also investigated for a silicone oil bridge.

2. EXPERIMENTAL APPARATUS AND INSTRUMENTATION

A schematic of the test section is shown in Fig. 1. It had upper and lower disks of 7.0 mm diameter made of brass. Details of the experimental apparatus and procedure can be found in a previous report[7].

2.1 Disk and Fluid Temperature Measurements

Thermocouples were used to accurately measure the individual disk temperatures, T_H and T_C, the disk temperature difference, ΔT, and liquid temperature, T_f. The liquid temperature fluctuations were measured using a type-T micro-thermocouple with a wire size of 25 μm inserted into the liquid bridge from the top through a small hole in the upper disk. To sample and record the temperature data nearly free of noise, a PC-based National

Instruments Data Acquisition System (Model PCI-6035E with SCXI-1102) was used. For the liquid temperature and ΔT measurements, high-gain, low-noise DC amplifiers (NEC Model 6L06H) were used to amplify the T/C signals before the data acquisition system to maximize the signal-to-noise ratio. All the temperature data were sampled using Labview software at a rate of 10 Hz, stored in files and graphically displayed in real-time.

In each run, the liquid was injected into the bridge to maximize the initial volume ratio and then the disk temperature difference, ΔT, was either increased or decreased by changing the temperatures of the cold and hot circulation baths connected to the upper and lower disks, and the voltage supplied to the Peltier element attached to the lower (cold) disk. The disk temperature difference, ΔT, was varied as slowly as possible at a relatively constant rate to cross the critical temperature difference and achieve transition from steady to oscillatory flow or vice versa before the volume ratio decreased to less than about 80 - 90% for the ramp increase cases. For step increases in ΔT, the temperatures of the lower and upper disks were set and held at certain values until a constant mean fluid temperature was reached. Fresh liquid was injected to overflow from the lower disk and renew the liquid bridge surface at the beginning of each measurement in order to avoid obtaining data with a contaminated liquid bridge surface.

2.2 Horizontal Vibration Tests

A PC-controlled vibration stage (Parker-Daedal Model 404XR150MP) was employed to apply horizontal vibrations to a liquid bridge and find the effect on ΔT_{cr} and the response of the free surface. The test section was mounted on the stage, which was translated horizontally at a specific frequency and amplitude. A video camera and a single-axis accelerometer were mounted on the same stage to monitor the liquid bridge motion and acceleration level, respectively. A laser displacement meter (Keyence Model LB1010) with a resolution of 2 μm was also used to measure the position of the test section in a fixed frame of reference.

During the experiment with acetone, the liquid evaporated from the free surface so that the ratio of the minimum liquid bridge diameter to the disk diameter (D_{min}/D) decreased continuously with time. However, for silicone oil the volume change of the liquid bridge during both stationary and vibration experiments was negligible.

3. RESULTS AND DISCUSSION

3.1 Oscillation Frequency Data for Stationary Acetone Bridges

Experiments were first conducted with an acetone liquid bridge and the temperature oscillation frequencies were determined for partially open and closed systems. Figure 2 shows a typical power spectrum of temperature oscillations for acetone in a closed system, which indicates two distinct peaks.

Figure 3 shows the dependence of the fundamental oscillation frequency on the disk temperature difference and aspect ratio for a closed system. The figure shows that the oscillation frequency increases nearly linearly with ΔT, and the oscillation frequency is proportional to the inverse of the aspect ratio. With the increasing aspect ratio, the slope of the frequency dependence on ΔT decreases. The frequency analysis was also performed for a partially open system. Figure 4 shows the dependence of the fundamental oscillation

frequency on ΔT and the aspect ratio. Comparing the frequencies for the closed and partially open systems, it is clear that for the partially open system the oscillation frequencies are about 20% greater than those obtained for the closed system at the same ΔT.

Based on numerical simulation results, Leypoldt et al.[8] proposed the following equation to describe the dependence of the temperature oscillation frequency in a liquid bridge on the disk temperature difference.

$$\omega^{TW} = 7.0 \times \varepsilon + 28.9 \quad (1)$$

where,

$$\omega = 2\pi f (H^2/\nu) \quad (2)$$

and

$$\varepsilon = (\Delta T - \Delta T_{cr}) / \Delta T_{cr} \quad (3)$$

Their numerical simulation was performed for a liquid bridge with an aspect ratio equal to unity, Prandtl number of 4 and Biot number of 0. The frequencies of the temperature oscillations in the acetone bridge for different aspect ratios are plotted in Figure 5 using the non-dimensional parameters defined by Leypoldt et al.[8] For an acetone bridge in a closed system with an aspect ratio of unity, the Prandtl number was 4.3 and the frequency data could be represented by the following equation:

$$\omega^{TW} = 7.8 \times \varepsilon + 43.5 \quad (4)$$

The fitted equation (Equation (4)) and the numerical simulation prediction (Equation (1)) have very similar slopes but different intercepts. The difference in the intercepts can be attributed to the different Biot numbers used in numerical simulation (Bi=0) and experimental data (Bi>0), although the evaporation rate was kept to a minimum by enclosing the liquid bridge with a quartz tube.

3.2 Horizontal Vibration Experiments

Effects of Vibration on ΔT_{cr} for Acetone Bridge

The test section was forced to vibrate sinusoidally at various frequencies and with different amplitudes. The temperature difference between the upper and lower disks was increased gradually. Figure 6 shows the fluid temperature fluctuations in an acetone liquid bridge vibrated at a frequency of 8 Hz and an acceleration level of 5 mg. Critical ΔT was determined following the same procedure described in our previous report.[7]

Figure 7 shows the effect of external vibration on the critical temperature difference data for acetone. It is evident from this figure that the external vibration had a negligible effect on the critical temperature difference for the acetone liquid bridge in the range of variables studied.

Surface Oscillations of an Acetone Bridge

The frequency of surface oscillations was also determined for an acetone bridge as shown in Figure 8. Interestingly, under different external vibration frequencies and for diameter ratios close to unity, a surface oscillation frequency of 12 Hz was obtained. Except for the case of 1 Hz, all other vibrating frequencies yielded the same surface oscillation frequency. From the figure it can be concluded that geometrical parameters of the liquid bridge play an important role.

For the acetone bridge the maximum surface oscillation amplitude was determined and the oscillation frequency was obtained for the maximum oscillation amplitude. Results are shown in Table 2 for the acceleration level of 5 mg. The frequency of maximum amplitude oscillations was not correlated with the external vibration frequency.

Surface Oscillation of an Isothermal Water Bridge

A water bridge was also tested to measure the response of the liquid bridge surface to external vibrations. The amplitude and frequency of vibration were varied for different diameter ratios with the maximum acceleration level kept at 25 mg. Figure 9 shows the surface oscillation amplitudes, which generally increased with the diameter ratio. Figure 10 shows a strong dependence of the maximum surface oscillation amplitude on the diameter ratio of the liquid bridge. For a constant diameter ratio, the surface oscillation amplitude peaked at some vibration frequencies, and the peak was the highest at the vibration frequency of 19 Hz, as shown in Figure 11.

A frequency analysis was performed to identify the most dominant frequency of surface oscillations in response to an external vibration. Table 1 shows the surface frequencies detected, which were much higher than the applied vibration frequencies and relatively independent of the vibration frequencies.

Modification of a Vibration Model

Ichikawa et al.[6] developed a simple spring-damper model for predicting the vibration frequency of a straight liquid cylinder responding to external vibrations. However, the liquid bridges are not perfectly cylindrical and as previously discussed, geometrical factors are quite important. Therefore, to include the geometry factor, a modified model applicable to a hyperboloid shape was developed.

Ichikawa et al.'s model starts with equation (5):

$$m\frac{d^2x}{dt^2} + 2mk\frac{dx}{dt} + m\omega_0{}^2 x = \frac{F_0}{m}\sin\omega t \tag{5}$$

where m, k, ω_0, ω, x, and F_0 are the moving mass of the liquid bridge, damping parameter, restoring force parameter, dimensionless vibration frequency, displacement of the free surface from the equilibrium position and magnitude of applied external force, respectively. Solving Equation (5) gives the following expressions for the surface oscillation amplitude and resonance frequency:

$$x_{amp.} = \frac{1}{\sqrt{(\omega_0{}^2 - \omega^2)^2 + 4k^2\omega^2}}\frac{F_0}{m} \tag{6}$$

$$\omega_{Res.} = \sqrt{\omega_0^{\,2} - 2k^2} \tag{7}$$

If the diameter ratio for a hyperboloid liquid bridge is defined as:

$$Q = \frac{D_{\min}}{D_{disc}} = \frac{R_{\min}}{R_{disc}} \tag{8}$$

then, the shape of the hyperboloid liquid bridge is given by:

$$\frac{x^2 + y^2}{R_{\min}^{\,2}} - \frac{z^2}{\dfrac{H^2}{4\left[\left(\dfrac{R_{disc}}{R_{\min}}\right)^2 - 1\right]}} = 1 \tag{9}$$

The following modified parameters were defined:
moving mass,

$$m = \frac{\pi \rho D_{disc}^{\,2} H}{12}(2Q^2 + 1) \tag{10}$$

restoring force parameter,

$$\omega_0 = \frac{4}{H}\sqrt{\left(\frac{\sigma}{D_{disc}\rho}\right)\left(\frac{3Q}{Q^2+1}\right)} \tag{11}$$

Solving Equation (5) with the modified parameters for the hyperboloid liquid bridge gives the following resonance frequency and amplitude:

$$f_{Res} = \frac{1}{2\pi H}\sqrt{\frac{16\,\sigma}{D_{disc}\,\rho}\,\frac{3Q}{2Q^2+1} - \frac{2v^2}{H^4}} \tag{12}$$

$$x_{amp} = \frac{a_0}{\sqrt{\left[\left(\dfrac{16}{H^2}\right)\left(\dfrac{\sigma}{D_{disc}\rho}\right)\left(\dfrac{3Q}{2Q^2+1}\right) - (2\pi f)^2\right]^2 + \dfrac{16\pi^2 v^2 f^2}{H^4}}} \tag{13}$$

A comparison between the model predictions and calculated surface oscillation frequencies from measurements are given in Table 3 for acetone and water. The model predictions are in good agreement with the measurements. Figure 12 shows the measured frequencies for the water bridge and the model predictions. The present model qualitatively predicts the trend of the data.

Silicone Oil Experiments: Effects of Vibrations on ΔT_{cr}

Experiments were also performed with a 5 cSt silicone oil, which has a higher Pr than

acetone and water but is not volatile and is less susceptible to surface contamination. The experiments were conducted with and without any external vibration applied to the liquid bridge by moving the test section sinusoidally in a horizontal direction using a PC-controlled translation stage.

For the stationary case, Figure 13 shows the fluid temperature oscillations, root mean square value of the temperature oscillations and the disk temperature difference for a stationary liquid bridge of 5 cSt silicone oil. By increasing the disk temperature difference, the amplitude of the temperature oscillations increased sharply at a certain value of ΔT, identified to be the critical ΔT. Thus, the critical temperature difference, ΔT_{cr}, was 24.7°C for AR=0.94 and disk diameter of 7 mm. The frequency spectrum showed no peaks for the steady flow state while two peaks appeared at frequencies of 0.48 Hz and 0.96 Hz, for the oscillatory case when the temperature difference exceeded the critical value.

The vibration experiments were conducted first by increasing the disk temperature difference gradually (ramp increase) and later in steps (step increase). For the ramp increase case, Figure 14 shows the frequency spectra for liquid temperature oscillations under the external vibration of 0.2 Hz and 0.26 mm amplitude. When the disk temperature difference was small and less than ΔT_{cr}, peaks appeared in the frequency spectrum at multiples of 0.2 Hz, with a large peak appearing at 0.6 Hz, corresponding to the third harmonic of the external vibration frequency. As soon as the temperature difference was increased to values greater than ΔT_{cr}, a peak at 0.48 Hz also appeared as in the stationary liquid bridge case.

Figure 15 shows the liquid temperature oscillations in response to a ramp increase in ΔT for the case of vibration amplitude and frequency set at 0.5 mm and 0.8 Hz, respectively. As shown in the Figure there was a continuous increase in the amplitude of temperature oscillations, and it was not possible to clearly determine ΔT_{cr} from the liquid temperature oscillations. Figure 16 shows the power spectrum for different portions of the data obtained for the case shown in Figure 15. Interestingly, the same frequency peak at 0.48 Hz appeared in a certain range of data and grew in magnitude. The first appearance of this frequency indicates the neighborhood of the critical temperature difference. The smaller the rate of ΔT increase, the narrower the neighborhood of the critical temperature difference would be.

To determine ΔT_{cr} more accurately, the disk temperature difference was increased in steps of 0.5 °C. After each step increase, temperature data were recorded for 150 s. Figure 17 shows the results of the step increase method for the forced vibration case with a frequency and amplitude of 0.8 Hz and 0.5 mm, respectively. Figure 18 shows the power spectra of the temperature oscillations for each step increase in ΔT. At low ΔT, a clear peak was detected at 0.8 Hz, corresponding to the frequency of the external vibration. However, in the third graph (sample # 3001-4500) a peak at 0.48 Hz appeared and grew in amplitude. This particular oscillation frequency is the same as that obtained in the stationary case. The step increase method allowed more reliable and accurate determination of ΔT_{cr} data for the vibrated liquid bridges.

Figure 19 shows the ΔT_{cr} data for different acceleration levels between 1.3 and 18 mg while the amplitude of external vibration was kept constant at 0.5 mm. This Figure clearly shows that ΔT_{cr} was unaffected by the external vibration. In Figures 20 and 21, the critical temperature difference data are shown for different acceleration levels under constant amplitudes of 1 and 3 mm, respectively. Again, no apparent effect of external vibrations on

ΔT_{cr} was observed.

Silicone Oil Experiments: Surface Oscillation

In response to the horizontal vibrations applied, the silicone oil bridge surface vibrated quite vigorously. The maximum amplitude of the surface oscillations under forced vibration occurred at the location of the minimum diameter of the liquid bridge, i.e., the thinnest part of the liquid bridge. Figure 22 shows the surface oscillation data for the 5 cSt silicone oil bridge under different vibration conditions. For the external vibration amplitude of 3 mm and frequency of 1 Hz, the surface oscillation amplitude was 50 μm for low disk temperature difference, $\Delta T < \Delta T_{cr}$, but increased to 75 μm at $\Delta T > \Delta T_{cr}$. The reason for this increase needs to be further investigated, however, it could be due to an increase in the average liquid temperature and thus a decrease in the viscosity and surface tension of the liquid bridge.

The volume ratio of the liquid bridge under different vibrating conditions was measured to determine if vibration causes any fluid loss due to drainage. Figure 23 shows that external vibration did not affect the volume ratio of the liquid bridge.

To get a better understanding of the liquid bridge surface response to external vibrations, the silicone oil bridge was forced to vibrate at different frequencies and with different amplitudes. A digital video camera was used to record the surface oscillation in a Lagrangian frame of reference. Figure 24 shows a sample image of the recorded vibrating liquid bridge. Edge detection software developed by NASDA was used to digitize the edge of the liquid bridge in different frames. The whole liquid bridge was in the view of the Hitachi CCD camera (Model VK-C370) and the frame rate was 30 frames/s. Due to the limited resolution of this camera, additional experiments were performed with a Megaplus camera (Model ES310), having a resolution of 600 x 480 pixels and capable of recording 124 frames per second directly on the hard disk of a PC. A set of extension rings and lenses was also used to get a greater magnification.

A thin Platinum wire with a known diameter of 225 μm was used to determine the scale for each pixel. A resolution of 5.8 μm per pixel was attained in the horizontal direction. The disk diameter for the experiments was 7 mm while the distance between the disks was 3.0 mm providing an aspect ratio of 0.86. Different vibration amplitudes (0.5 ~ 2.0 mm) and frequencies (0.5 ~ 2.0 Hz) were used to cover a range of accelerations (0.5 ~ 2.0 mg). Figure 25 shows one of the frames recorded by the Megaplus camera. Edge detection software accepted the image as input and provided digitized edge coordinates in an output file.

Figure 26 shows the surface positions at different elevations of the liquid bridge. This figure clearly shows that the surface fluctuations grew in amplitude further down from the hot (upper) disk. The figure also shows that close to the hot corner, increasing the disk temperature difference from 0 to a value higher than ΔT_{cr} increased the fluctuation amplitude of the liquid bridge surface. This could be due to higher temperatures near the hot disk and thus lower viscosity and surface tension of the liquid. The figure also suggests that the frequency of the surface fluctuations is greater than the applied frequency. Figure 27 shows the surface fluctuations for another vibration condition.

The current motorized linear stage uses a ball screw and linear bearings that have a small coefficient of friction. A very sensitive laser displacement sensor was used to measure the displacement of the stage with a resolution of 2 μm. A very sensitive accelerometer (Dytran

Model 3191A1) was later used to measure the actual acceleration levels of the stage movements. Figure 28 shows the output signals from the displacement sensor and accelerometer collected simultaneously. Data obtained with the laser displacement sensor showed a very smooth, near-sinusoidal movement of the stage, however, the accelerometer data showed larger chaotic accelerations than what had been expected. This surprising result could be due to the friction in the driving mechanism of the stage. Thus, another vibrating linear stage with a smooth, friction-free movement such as an air-bearing stage should be used in future experiments.

CONCLUSIONS

In acetone liquid bridges with D = 7 mm and various aspect ratios, the temperature oscillation frequency increased nearly linearly with the disk temperature difference. Also, the frequency of temperature oscillations was found to be proportional to the inverse of the aspect ratio. Increasing the aspect ratio of the liquid bridge reduced the slope of the frequency increase with ΔT. For the partially open system, the oscillation frequencies were about 20% greater than those determined for the closed system at the same ΔT. The variation of the temperature oscillation frequency in acetone liquid bridge was compared with Leypoldt et al.'s numerical predictions[8]. The trend of the variation of the temperature oscillation frequency was in qualitative agreement with that predicted by the numerical simulation.

The acetone liquid bridge was forced to vibrate with different amplitudes and frequencies and the critical temperature difference data were obtained. Vibration did not have any effect on the critical temperature difference for acetone.

Water was also used to form an isothermal liquid bridge between two 7 mm disks and vibrated with different amplitudes and frequencies. The surface oscillation amplitude was found to be dependent on the diameter ratio of the liquid bridge. The surface of the liquid bridge oscillated with a frequency much larger than the frequency of the applied vibration and seemed to be independent of the frequency of applied vibration. Ichikawa et al.'s model[6] was modified to predict the resonance frequency of a hyperboloid-shaped liquid bridge. The predictions of the modified model showed qualitative agreement with the measurements.

Experiments were also conducted using a 5 cSt silicone oil bridge between two 7 mm diameter disks. The critical temperature difference for a stationary (non-vibrated) liquid bridge with an aspect ratio of 0.94 was 24.7 ^{o}C, and the temperature oscillation frequency was 0.48 Hz. The same silicone oil bridge was vibrated under different amplitudes and frequencies. For a vibrating liquid bridge, determining the critical temperature difference in a ramp increase in temperature difference was only possible by making use of a frequency analysis. Uncertainties, however, could be large depending on the rate of increase in the temperature difference. Therefore, a step increase method was adopted to obtain more accurate ΔT_{cr} data. The critical temperature difference was then measured for the silicone oil bridge vibrated at different acceleration levels, but no apparent effect of vibration could be observed on the critical temperature difference in the range of variables covered.

For the vibrating liquid bridge, greater amplitudes of surface oscillation were measured when the disk temperature difference was greater than the critical value compared to an isothermal liquid bridge. Analyses of images obtained under different vibration amplitudes and frequencies showed that the surface oscillation amplitude increased with the distance below the hot corner.

REFERENCES

[1] Plekasis, N. A., Economou, K., and Tsamopoulos, J.A.: "Linear oscillations and stability of a liquid bridge in an axial electric field", Physics of Fluids, Vol.13 (12) (2001), pp.3564 -3581.

[2] Nicolas, J.A., Rivas, D. and Vega, J.M.: "On the steady streaming flow due to high-frequency vibration in nearly inviscid liquid bridges", J. Fluid Mechanics, Vol. 354, (1998), pp.147-174.

[3] Preisser, F., Schwabe, D. and Scharmann, A.: "Steady and oscillatory thermocapillary convection in liquid columns with free cylindrical surface", J. Fluid Mechanics, Vol.126, (1983), pp.545-567.

[4] Velten, R., Schwabe, D. and Scharmann, A.: "The periodic instability of thermocapillary convection in cylindrical liquid bridges", Physics of Fluids A, Vol. 3(2)(1991), pp. 267-279.

[5] Kamotani, Y., Ostrach, S. and Vargas, M.: "Oscillatory thermocapillary convection in a simulated float-zone configuration", J. Crystal Growth, Vol. 66 (1984), pp. 83- 90.

[6] Ichikawa, N., Misawa, M. and Kawaji, M.: "Resonance behavior of liquid bridge caused by small vibration", Proc. of 4th International Conference on Multiphase Flow, New Orleans, Louisiana, USA. May 27 – June 1, 2001.

[7] Kawaji, M., Otsubo, F., Simic, S. and Yoda, S.: "Transition to oscillatory Marangoni convection in liquid bridges of intermediate Prandtl number", Annual Report on Marangoni Convection Modeling Research, NASDA Technical Memorandum, December 2001, National Space Development Agency of Japan, pp. 107-132.

[8] Leypoldt, J., Kuhlmann, H. and Rath, H.J.: "Three dimensional numerical simulation of thermocapillary flows in cylindrical liquid bridges", J. Fluid Mechanics, Vol. 414 (2000), pp. 285-314.

Table 1. Measured surface oscillation frequency under different applied vibrations for water bridge, $D_{min}/D=1.0$

APPLIED VIBRATION FREQUENCY (Hz)	SURFACE OSCILLATION FREQUENCY (Hz)
1	20
2	20
3	21
4	20
5	20
6	18
7	21

Table 2. Surface oscillation frequency (in Hz) at maximum free surface oscillation amplitude (Acetone, acceleration level = 5mg, H/R = 1.04)

FREQUENCY OF APPLIED VIBRATION (Hz)	SURFACE OSCILLATION FREQUENCY AT MAXIMUM AMPLITUDE
1	13
2	10
3	9
4	12
5	10
6	12
7	7
8	8
9	9
10	10
11	11
12	12

Table 3. Comparison of the measured resonance frequency with model predictions

	Model Prediction	Experimental
Acetone	11.2 Hz	4 and 12 Hz ($D_{min}/D = 0.76$)
Water	20.8 Hz	19 Hz ($D_{min}/D = 1$)

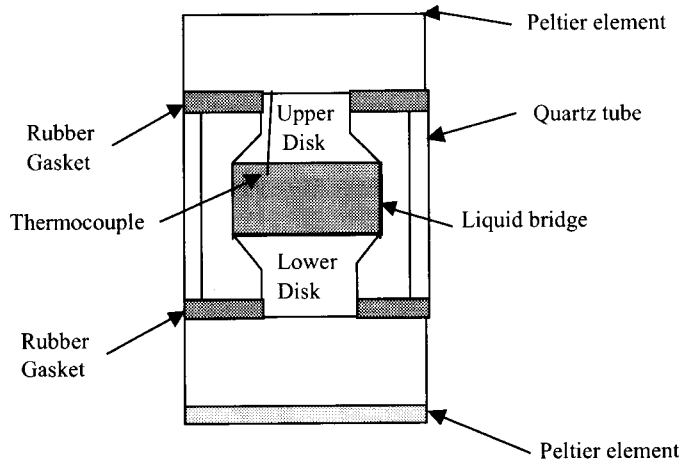

Figure 1. Schematic of the test section

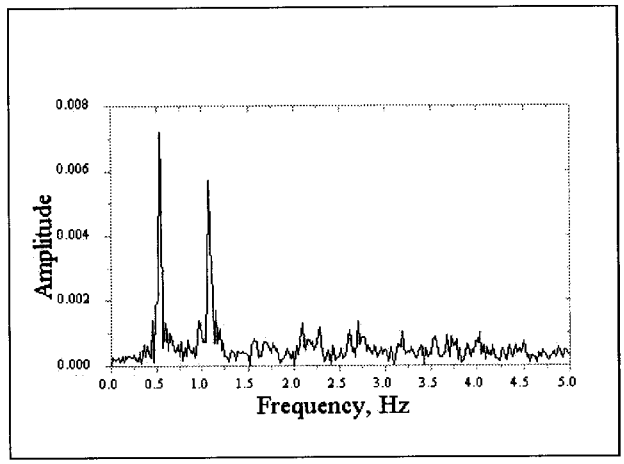

Figure 2. A typical power spectrum for acetone in a closed system: A= 0.84, ΔT= 2.85 K

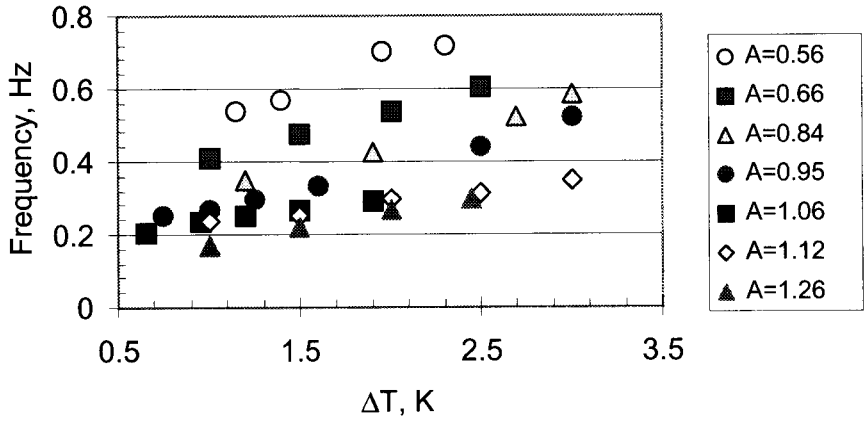

Figure 3. Main oscillation frequency for acetone in a closed system

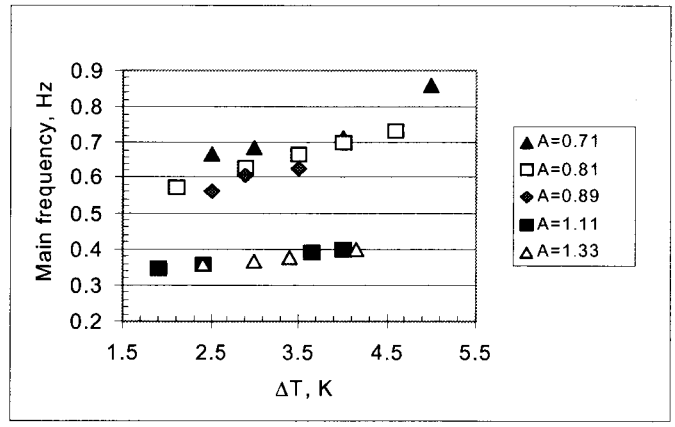

Figure 4. The main temperature oscillation frequency for acetone in a partially open system

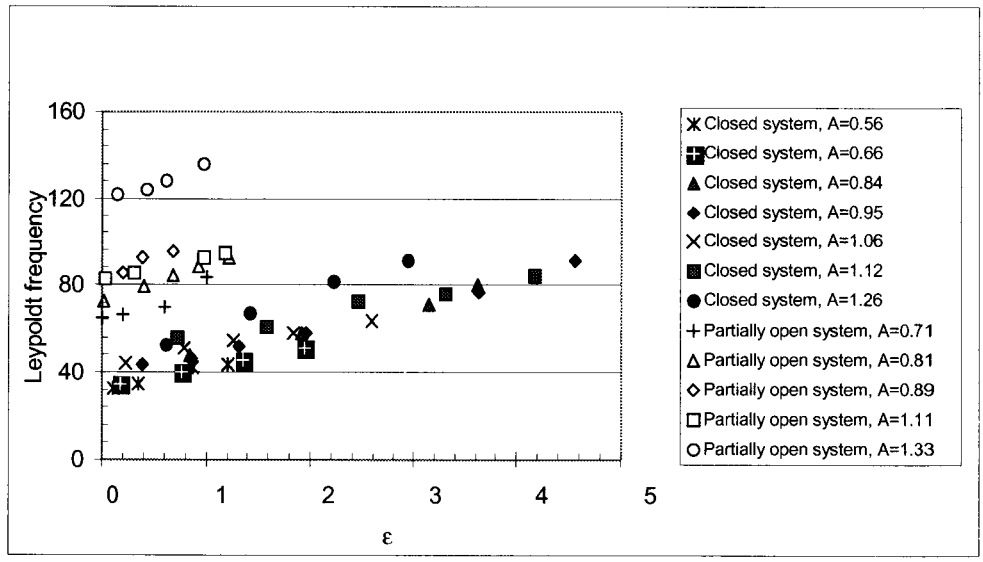

Figure 5. Frequency of the temperature oscillations in an acetone bridge

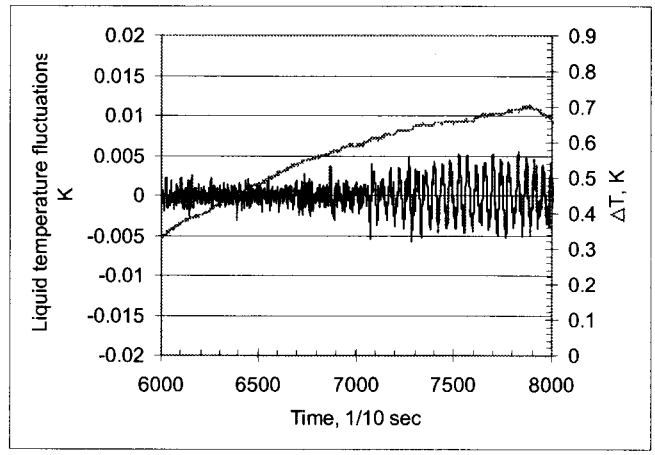

Figure 6. Acetone bridge temperature fluctuations under 8 Hz / 5 mg vibration

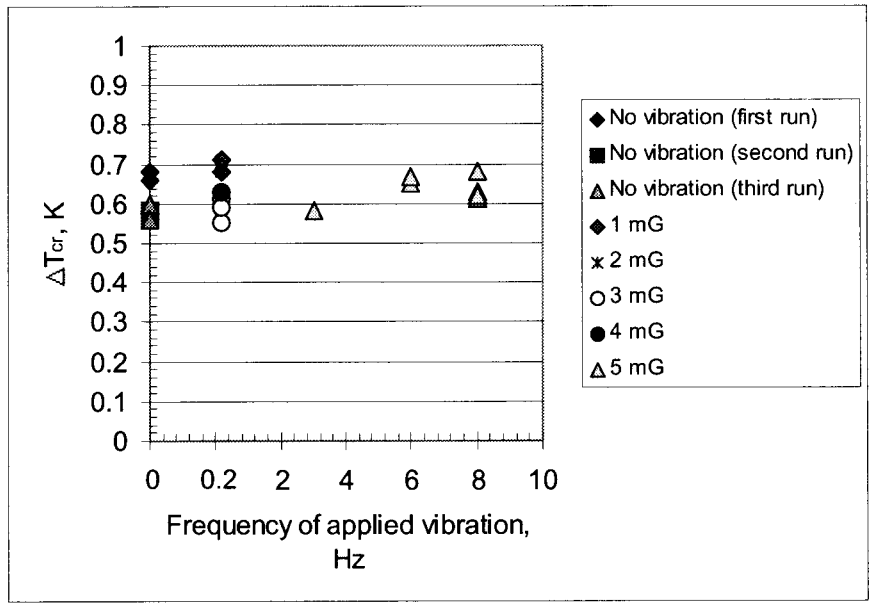

Figure 7. Effect of applied vibration on the critical temperature difference

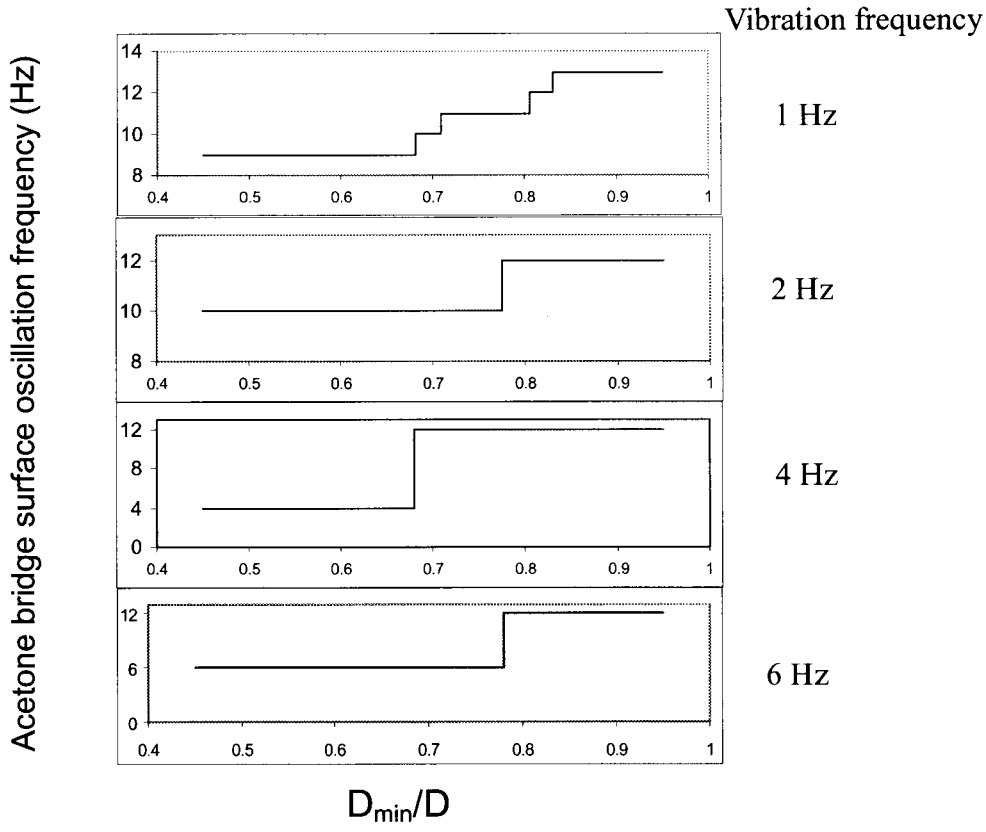

Figure 8. Frequency of surface oscillation for an acetone bridge under different external vibrations

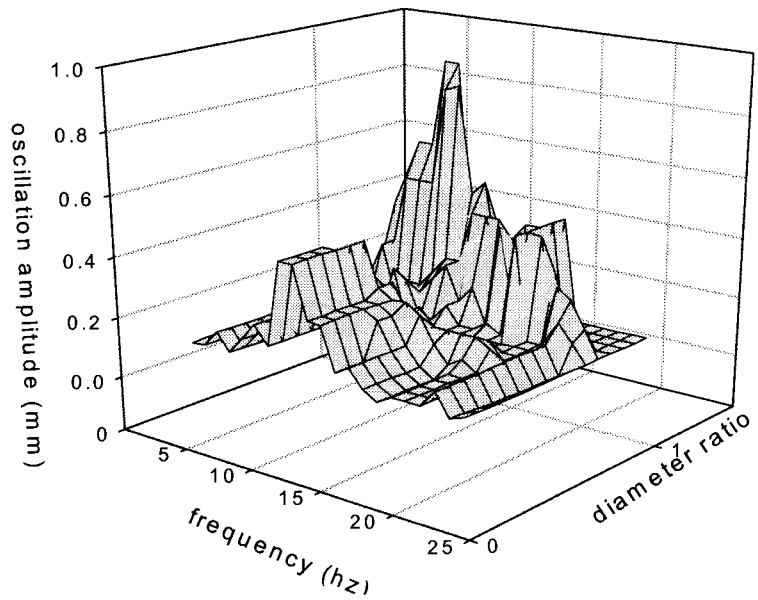

Figure 9. Surface oscillation amplitudes for a water bridge with a 25 mg maximum acceleration

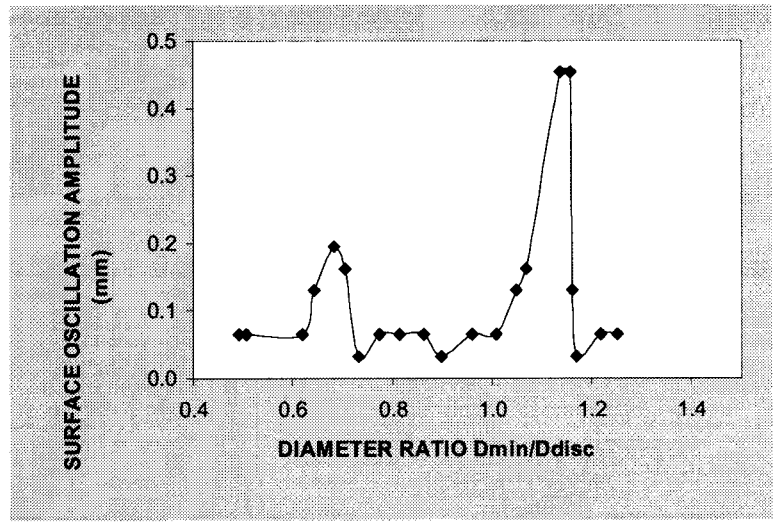

Figure 10. Dependence of surface oscillation amplitude on the diameter ratio of a water bridge

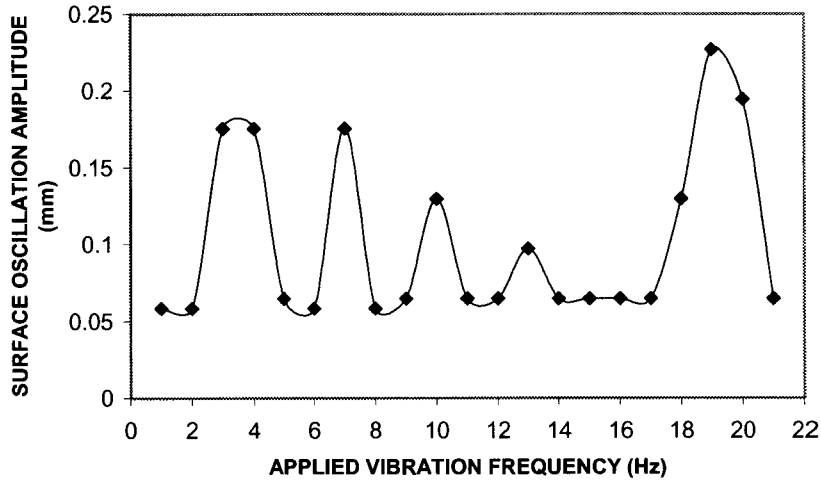

Figure 11. Surface oscillation amplitude under applied vibration for a water bridge

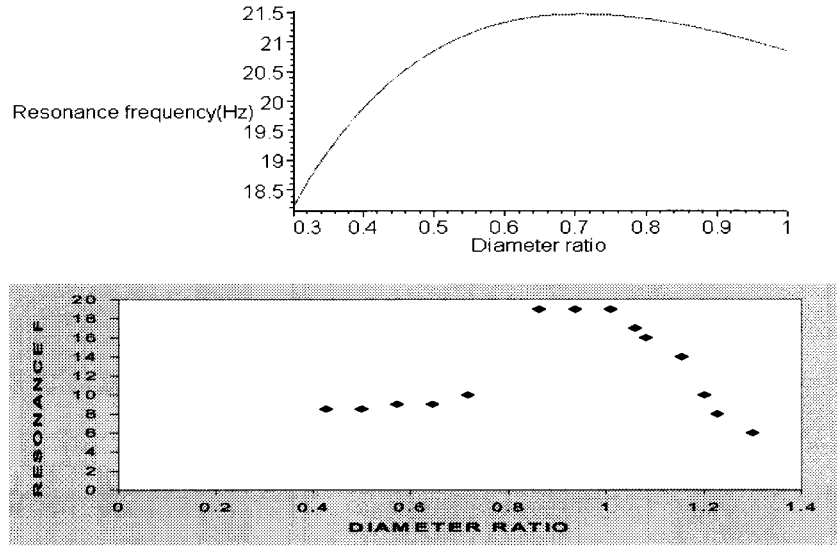

Figure 12. Predicted and measured surface oscillation frequencies for a water bridge

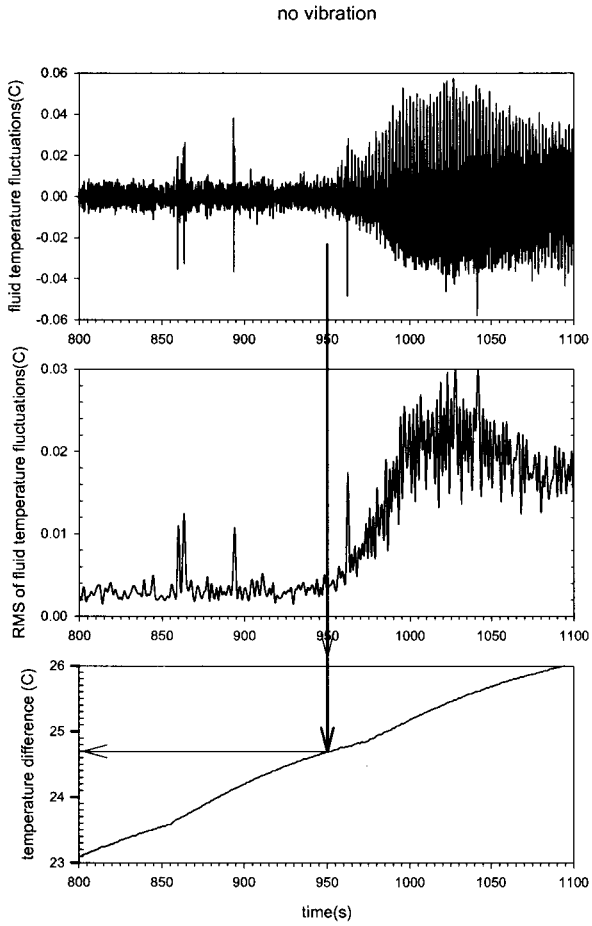

Figure 13. Fluid temperature oscillations, RMS of temperature oscillations and disk temperature difference for a stationary 5 cSt silicone oil bridge

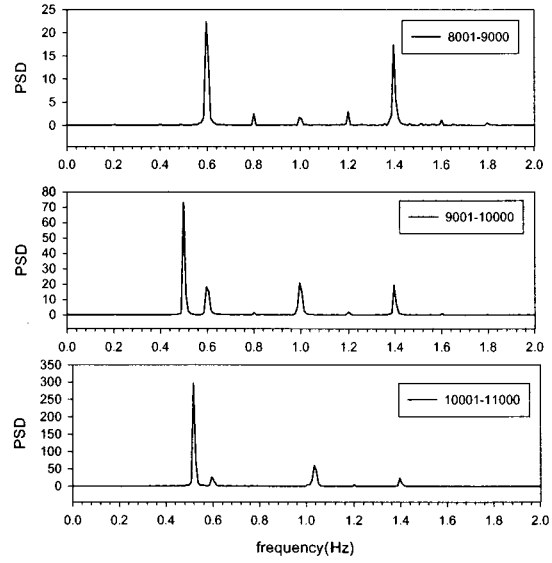

Figure 14. Frequency spectra of liquid temperature oscillations under external vibration at 0.2 Hz and 0.26 mm amplitude

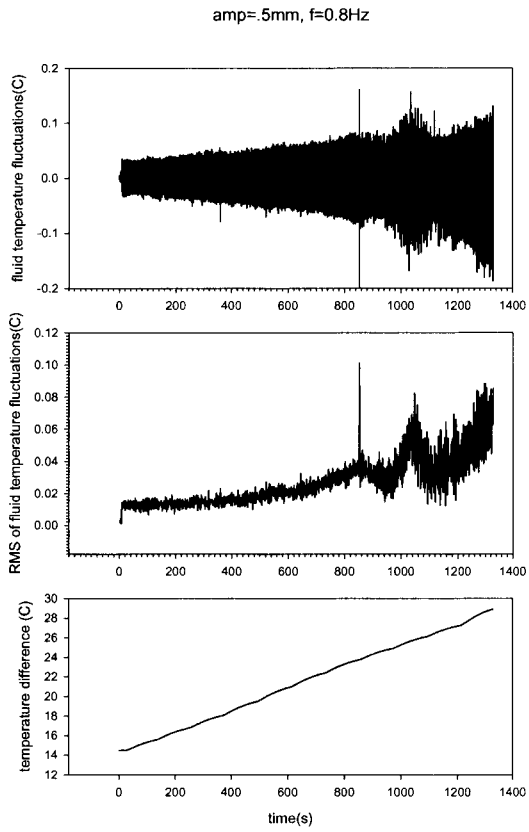

Figure 15. Response of the liquid temperature to a ramp increase for a vibrated silicone oil bridge (Amp=0.5mm, f=0.8 Hz)

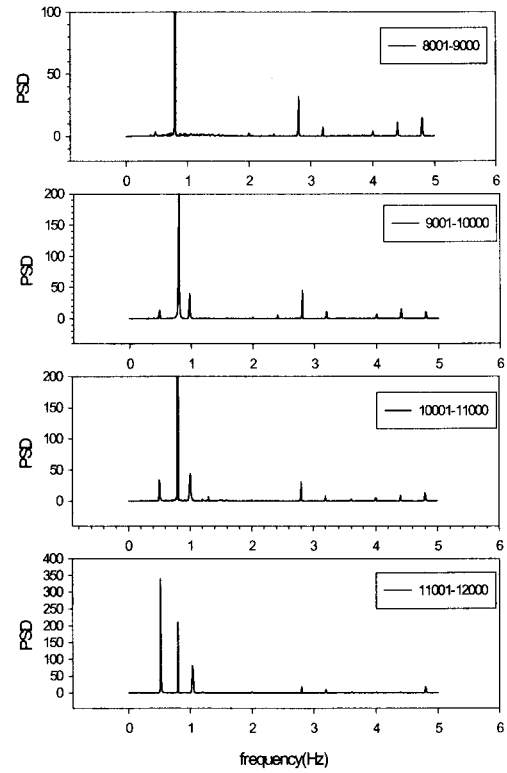

Figure 16. Power spectrum for a vibrated silicone oil bridge

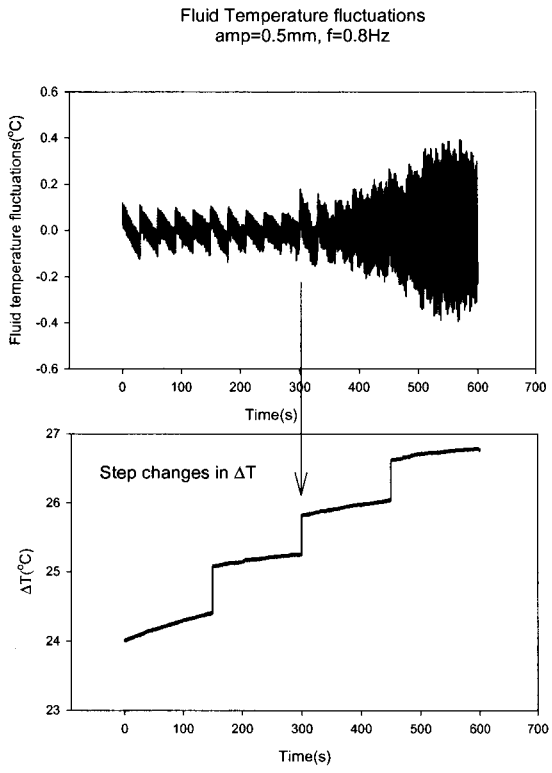

Figure 17. Step increase in ΔT for silicone oil bridge

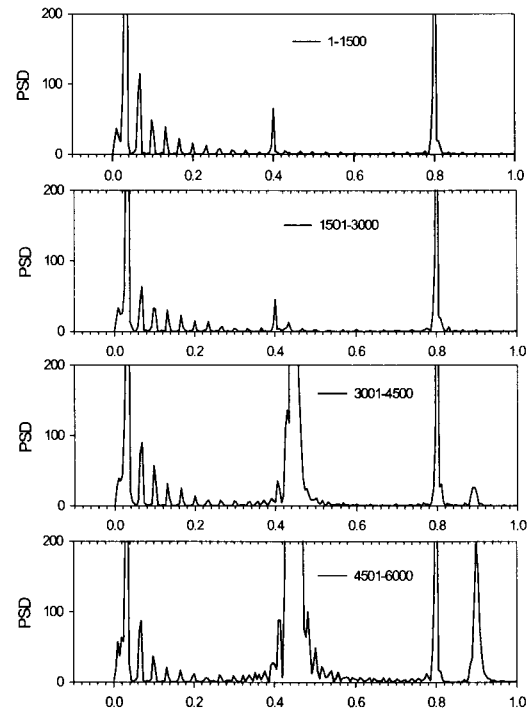

Figure 18. Power spectra of temperature oscillations for step increase in ΔT (for the data of Figure 17)

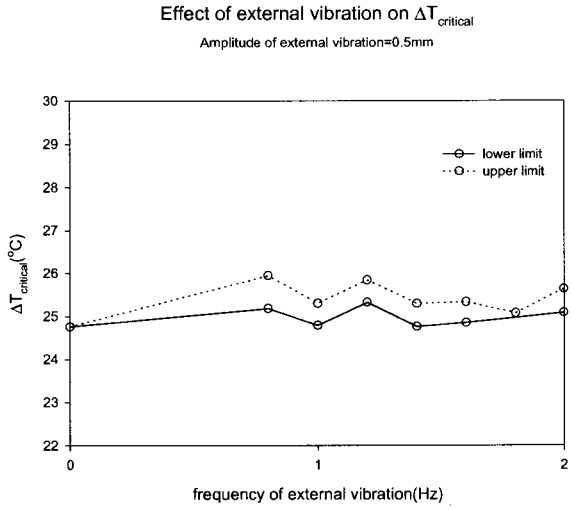

Figure 19. Critical disk temperature difference as a function of vibration frequency for silicone oil with vibration amplitude kept constant at 0.5 mm

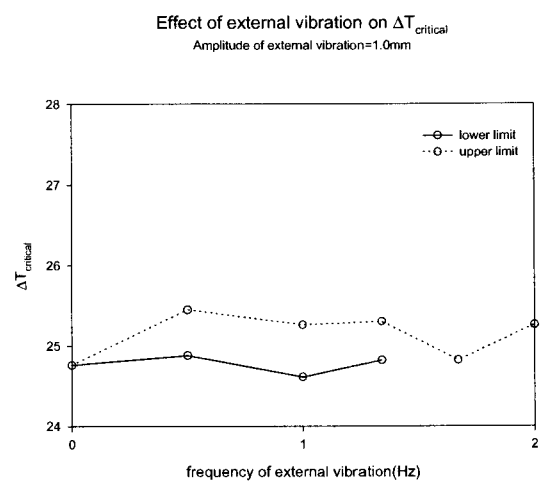

Figure 20. Critical disk temperature difference as a function of vibration frequency for silicone oil with vibration amplitude kept constant at 1.0 mm

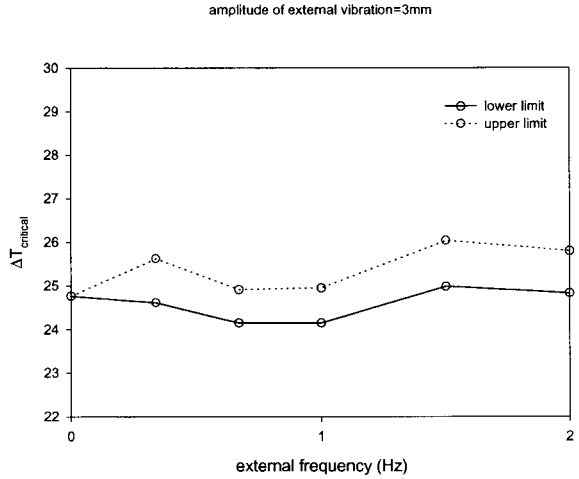

Figure 21. Critical disk temperature difference as a function of vibration frequency for silicone oil with vibration amplitude kept constant at 3.0 mm

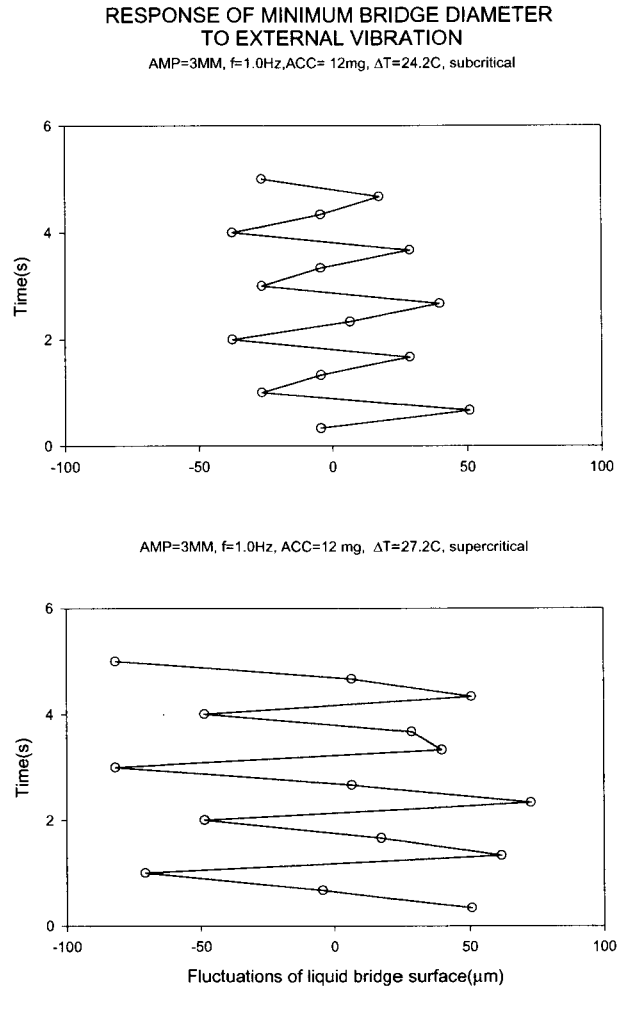

Figure 22. Surface oscillations of a silicone oil bridge

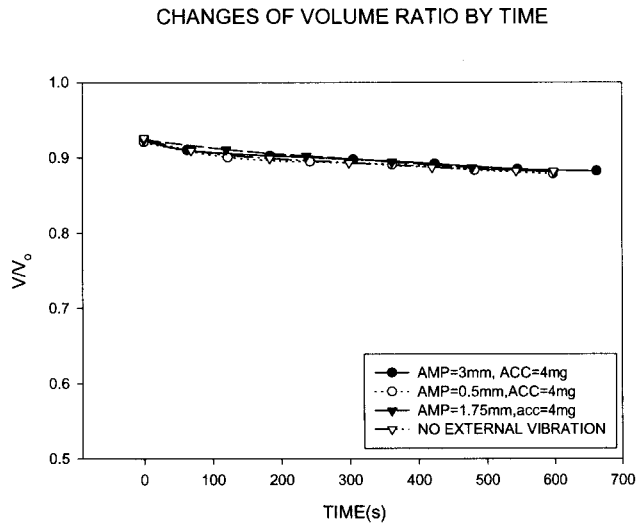

Figure 23. Volume ratio as a function of time for different vibration conditions

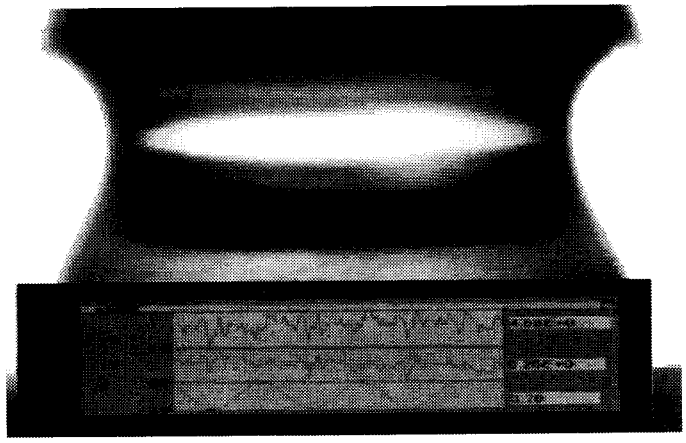

Figure 24. Sample image of a vibrating liquid bridge. Blue line shows the output of edge detection software

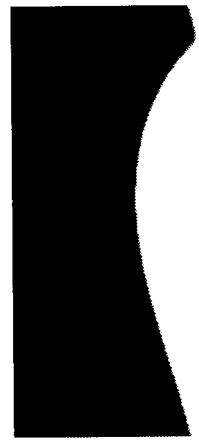

Figure 25. Sample image of a vibrating liquid bridge recorded by Megaplus camera

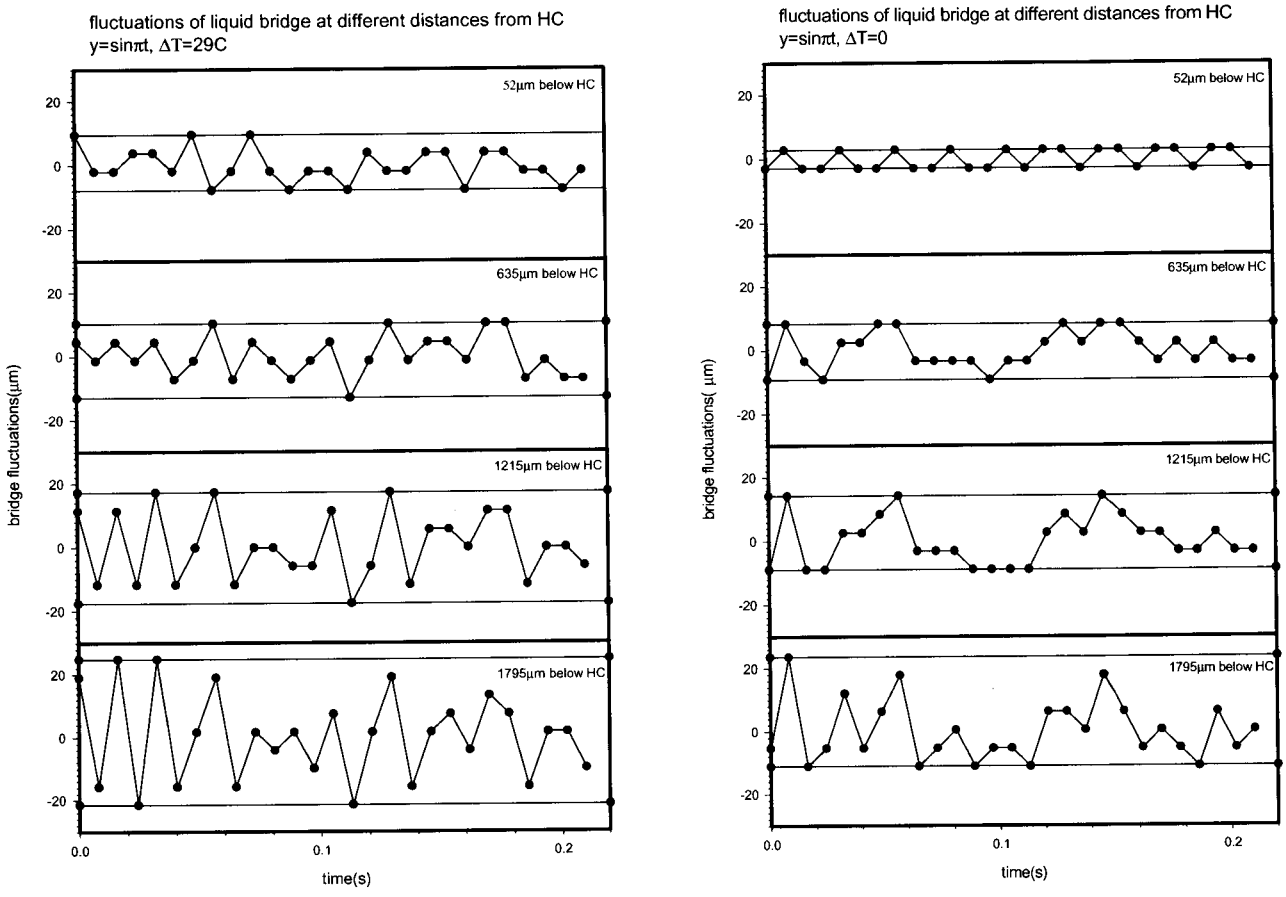

Figure 26. Surface fluctuations at different vertical positions below the hot corner of a silicone oil bridge

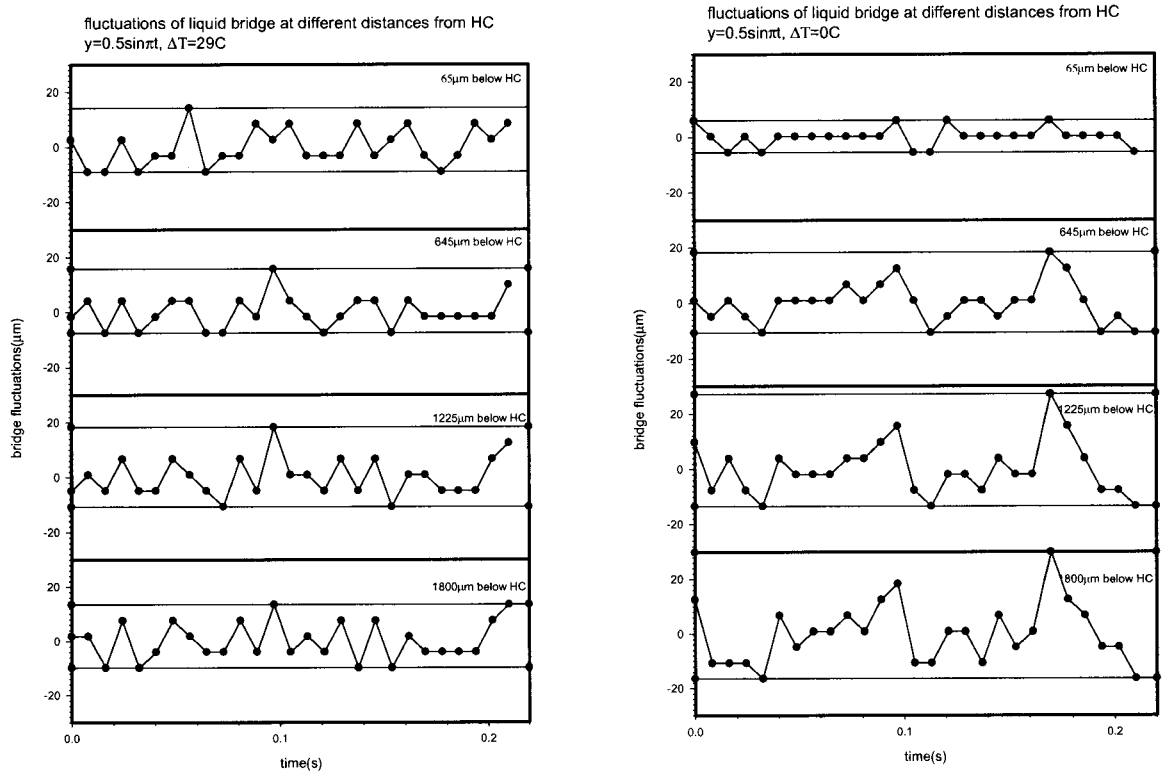

Figure 27. Surface fluctuations at different positions below the hot corner of a silicone oil bridge

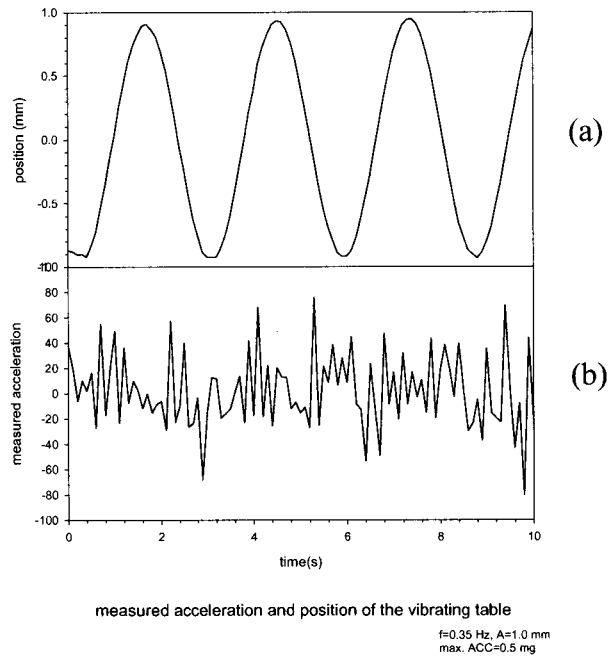

Figure 28. Output signals from the displacement sensor (a) and accelerometer (b)